Modeling probability and additive summation for detection across multiple mechanisms under the assumptions of signal detection theory

Frederick A. A. Kingdom McGill Vision Research, Department of Ophthalmology, Montreal, Quebec, Canada

Alex S. Baldwin McGill Vision Research, Department of Ophthalmology, Montreal, Quebec, Canada

Gunnar Schmidtmann McGill Vision Research, Department of Ophthalmology, Montreal, Quebec, Canada

Many studies have investigated how multiple stimuli combine to reach threshold. There are broadly speaking two ways this can occur: additive summation (AS) where inputs from the different stimuli add together in a single mechanism, or probability summation (PS) where different stimuli are detected independently by separate mechanisms. PS is traditionally modeled under high threshold theory (HTT); however, tests have shown that HTT is incorrect and that signal detection theory (SDT) is the better framework for modeling summation. Modeling the equivalent of PS under SDT is, however, relatively complicated, leading many investigators to use Monte Carlo simulations for the predictions. We derive formulas that employ numerical integration to predict the proportion correct for detecting multiple stimuli assuming PS under SDT, for the situations in which stimuli are either equal or unequal in strength. Both formulas are general purpose, calculating performance for forced-choice tasks with *M* alternatives, *n* stimuli, in *Q* monitored mechanisms, each subject to a non-linear transducer with exponent τ. We show how the probability (and additive) summation formulas can be used to simulate psychometric functions, which when fitted with Weibull functions make signature predictions for how thresholds and psychometric function slopes vary as a function of τ, *n*, and *Q*. We also show how one can fit the formulas directly to real psychometric functions using data from a binocular summation experiment, and show how one can obtain estimates of τ and test whether binocular summation conforms more to PS or AS. The methods described here can be readily applied using software functions newly added to the Palamedes toolbox.

Introduction

The early visual system contains tuned mechanisms that respond to particular stimulus features at particular locations in the visual field. For example, simple cells are sensitive to luminance modulations of some specific frequency, orientation, and phase. Behaviorally, however, the stimuli that are ecologically relevant are not the simple features that these mechanisms are sensitive to. More complex stimuli are the norm, and to represent these the visual system must combine the outputs of the simpler mechanisms. This leads to one of the most basic questions in vision science: How are these outputs combined? Numerous studies have addressed this "summation" question. It can be posed at any level of the brain from the basic summation of contrast signals (e.g., Hoekstra, Van der Goot, Van den Brink, & Bilsen, 1974) to the summation of semantic information between different modalities (e.g., visual and auditory stimuli in To, Baddeley, Troscianko, & Tolhurst, 2011), and there is no reason to expect the answer to be the same at every level and in every modality (although some degree of commonality would be parsimonious).

There are two ways in which experiments are typically conducted to investigate summation. In the first method, detection thresholds for two component stimuli, here termed "A" and "B," are measured. These can then be used to predict the threshold for the compound stimulus "A+B" (e.g., Baldwin, Husk, Meese, & Hess, 2014; Graham & Nachmias, 1971; Graham & Robson, 1987; reviewed by Graham, 1989;

Citation: Kingdom, F. A. A., Baldwin, A. S., & Schmidtmann, G. (2015). Modeling probability and additive summation for detection across multiple mechanisms under the assumptions of signal detection theory. *Journal of Vision*, *15*(5):1, 1–16, http://www.journalofvision.org/content/15/5/1, doi:10.1167/15.5.1.

doi: 10.1167/15.5.1 Received November 11, 2014; published April 17, 2015 ISSN 1534-7362

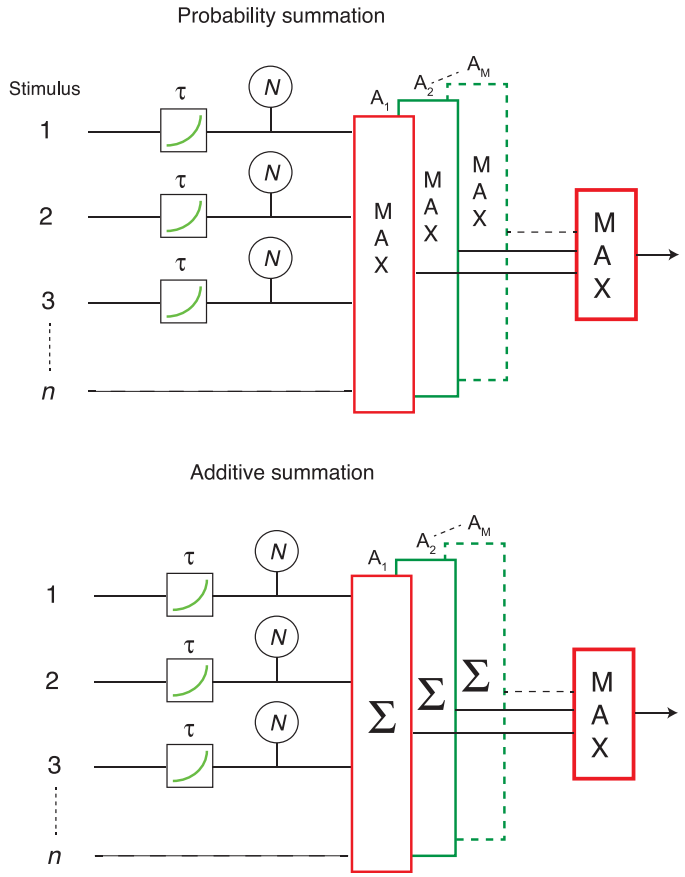

Figure 1. The two broad classes of summation considered within a signal detection theory framework. Top: PS; bottom: AS. N = addition of internal noise, n = number of stimuli, τ = exponent on transducer function. A_1 is the target alternative/interval, while A_2–A_M are the non-target (i.e., noise-alone alternatives/intervals) with M being the total number of alternatives/intervals in the forced-choice task. MAX = MAX decision rule.

Meese, 2010; Pirenne, 1943; Quick, Mullins, & Reichert, 1978; Sachs, Nachmias, & Robson, 1971). Different summation rules will make different predictions for the A+B threshold, and so the results from the experiment can be used to distinguish between them. The second method is similar; instead of using component versus compound stimuli the comparison is instead made between stimuli that "grow" along some dimension (e.g., increase in size). In terms of how the previous method was described, this can be thought of as obtaining thresholds for A, A+B, A+B+C, and so on (e.g., Bell & Badcock, 2008; Dickinson, Han, Bell, & Badcock, 2010; Dickinson, McGinty, Webster, & Badcock, 2012; Loffler, Wilson, & Wilkinson, 2003; Meese & Summers, 2012; Meese & Williams, 2000; Robson & Graham, 1981; Rovamo, Luntinen, & Näsänen, 1993; Schmidtmann, Kennedy, Orbach, & Loffler, 2012; Tan, Dickinson & Badcock, 2013). Again, different summation rules make different predictions for how thresholds change with the number of components.

Attention Window	Transducer	Single component	Multiple components	SS
Matched ($Q = n$)	Linear	$d' = gs$	$d' = gs\sqrt{n}$	$\alpha \propto \frac{1}{\sqrt{n}}$
	Non-linear ($\tau \neq 1$)	$d' = (gs)^{\tau}$	$d' = (gs)^{\tau}\sqrt{n}$	$\alpha \propto \frac{1}{\sqrt[\tau]{n}}$
Fixed ($Q > n$)	Linear	$d' = gs$	$d' = \frac{n(gs)}{\sqrt{Q}}$	$\alpha \propto \frac{1}{\sqrt{n}}$
	Non-linear ($\tau \neq 1$)	$d' = (gs)^{\tau}$	$d' = \frac{n(gs)^{\tau}}{\sqrt{Q}}$	$\alpha \propto \frac{1}{\sqrt[\tau]{n}}$

Table 1. Calculation of d' and summation slope (SS) for four models of additive summation. *Notes*: The number of stimulus components is given by n, the stimulus strength of each component by s, the input gain of the mechanism sensitive to that component by g, and the exponent of the mechanism's transducer by τ. Summation slopes indicate how thresholds α decline as a function of n, assuming all component thresholds are equal.

Experiments using multiple stimuli can be used to distinguish within and between two broad classes of summation model: additive summation (AS) and probability summation (PS), as illustrated in Figure 1. AS implies that the responses from the individual component mechanisms are summed together by a mechanism that is sensitive to the compound stimulus. This results in predictions that are relatively straightforward (see Table 1). For example, in the special case of linear summation, one predicts an inverse proportional relationship between the number of stimulated component mechanisms and threshold. With PS on the other hand, which is the main focus of this communication, there is no summation of the component signals into a mechanism sensitive to the compound stimulus. Rather, adding more stimuli improves performance because there is a greater chance that any one of the stimuli will be detected. Some investigators have considered whether some combination of AS and PS might underlie detection (e.g., Meese & Summers, 2012). However, for this communication we will only deal with the predictions from one or another of the standard forms of AS and PS.

When a PS model is tested it is frequently derived under the assumptions of high threshold theory (HTT; see Graham, 1989; Sachs et al., 1971). Under HTT the component mechanisms will be activated if their input exceeds some fixed threshold value. This threshold is assumed to be sufficiently high that it is only very rarely surpassed by the system's internal noise on its own. The component mechanisms in HTT have a binary response; they are either activated or not activated (though one must bear in mind that a weak signal may be insufficient to reach threshold in which case the

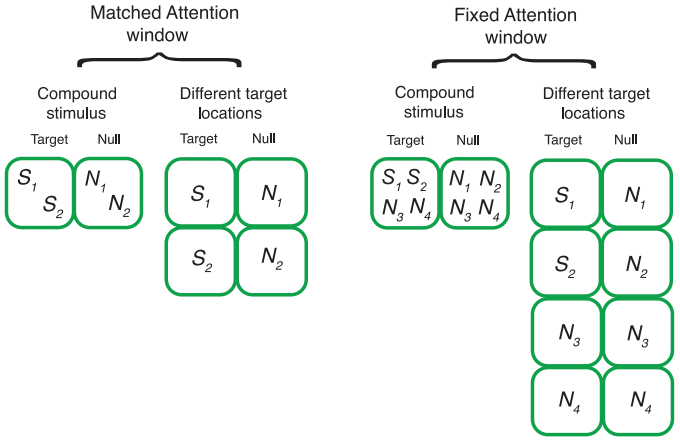

Figure 2. Schematic showing different summation scenarios for a two-interval forced-choice task ($M = 2$) with the target interval containing two stimuli S_1 and S_2. N_1–N_4 signifies internal noise in the channels/locations sensitive to the stimuli. Each green box denotes a spatial location. In the Matched Attention Window scenario on the left, irrespective of whether the two stimuli are presented in the same or different spatial locations, the observer attends to both channels sensitive to the stimuli or locations that contain the stimuli. For this situation $n = Q = 2$, where n is the number of stimuli and Q the number of monitored channels/locations. In the Fixed Attention Window scenario on the right, the observer attends to four channels/locations, even though only two stimuli are present. For this situation $n = 2$ and $Q = 4$.

observer guesses). Altogether this means that there is almost no "penalty" under HTT for monitoring additional non-target mechanisms, as any irrelevant internal noise carried by those mechanisms will have a vanishingly small effect on performance. This property of the HTT–PS model affects how researchers design their experiments. Specifically, there is no practical difference in the HTT–PS prediction between experiments that interleave their different summation conditions and those that block those conditions. Interleaving or blocking, however, *does* affect thresholds, at least for contrast grating detection (Meese & Summers, 2012), unfortunately for HTT.

The other form of the PS model is the one formulated under signal detection theory, or SDT (Green & Swets, 1966). Briefly, the component mechanisms under SDT give a continuous response to the presented stimulus, which is then perturbed by independent internal noise. The SDT–PS model takes the response from the most activated mechanism and uses that to make a decision about the stimulus (for example, by comparing the maximum response from each of two intervals to determine which contained the target). The internal noise in the non-target interval plays a significant role in the predictions made by the SDT–PS model, as there is no sensory threshold to squelch it. Because of this, whether the experimenter blocks or interleaves the different summation, conditions will make a significant difference to the SDT–PS model prediction (as the additional internal noise from the irrelevant monitored mechanisms in the interleaved case will degrade performance). When the conditions are blocked, the observer can focus attention only on the relevant channels, termed here the "Matched Attention Window" scenario. On the other hand, when the conditions are interleaved, the observer will likely monitor all potentially relevant channels, which means that the observer will also monitor the channels that only contain internal noise. Tyler and Chen (2000) coined the term "Fixed Attention Window" for this scenario. The difference between Matched and Fixed Attention Window scenarios is illustrated in Figure 2. The figure also illustrates three of the variables that are key to the expositions in this communication: Q is the total number of monitored channels/mechanisms on each trial; n is the number of those mechanisms that are activated by the target stimuli; and M is the number of intervals that are presented on each trial (e.g., an M of 2 gives a two-interval forced-choice task like that shown in Figure 2).

There is strong evidence that SDT is a better model of detection than HTT (Green & Swets, 1966; Laming, 2013; Nachmias, 1981). The widespread use of the HTT–PS model may therefore be surprising—however, there may be a number of reasons for this. First, the mathematical basis for calculating PS under the assumptions of SDT is more complex than with HTT. Current expositions of the equations involved are not fully generalized across n, Q, and M and are often daunting to the non-mathematician. Moreover, the predictions made by the existing theoretical papers on PS under SDT are not always presented as sufficiently different to those formulated under HTT-PS for authors to reconsider their choice of model. One aim of this paper is to reiterate what some investigators have already pointed out (e.g., Meese & Summers, 2012; Tyler & Chen, 2000), namely that there are significant differences between the two PS models both in terms of threshold predictions and, as importantly, predictions for the slopes of psychometric functions. An additional limitation of previous theoretical expositions is that they do not always incorporate a term for a non-linear transducer function, whereas many studies point to an accelerating transducer at threshold (Heeger, 1991; Legge & Foley, 1980; Meese & Summers, 2009, 2012; Tanner & Swets, 1954). Here we use τ as the exponent on stimulus intensity to embody a non-linear transducer, with $\tau > 1$ for an accelerating transducer.

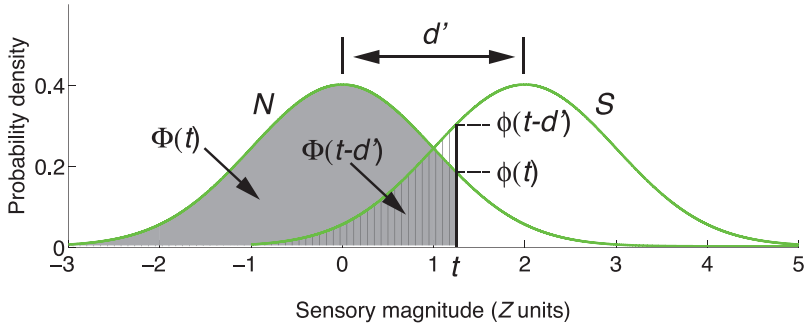

Figure 3. Parameters for calculating AS and PS under the assumptions of SDT. N = noise distribution; S = stimulus (or signal) distribution; t = sample sensory magnitude; d' = separation between noise and signal distributions; $\Phi(t)$ and $\Phi(t - d')$ are the areas under the noise and signal distributions to the left of t; $\phi(t)$ and $\phi\ (t - d')$ are the heights of the noise and signal distributions at t. Based on figure 6.5 in Kingdom and Prins (2010).

The relatively few researchers who *have* used an SDT–PS model tend to use Monte Carlo simulations rather than an analytic solution (e.g., Meese & Summers, 2012). Although the Monte Carlo method is simple to implement and will converge to an accurate prediction given sufficient processing time, it is markedly less efficient than an equation, even if the equation requires numerical integration for its solution. Execution speed is not an issue when a single calculation is required, but for the modeling in this communication, which involves many thousands of calculations in order to fit multiple psychometric functions and determine bootstrap errors of the fitted parameters and model goodness-of-fits, Monte Carlo simulations are prohibitively slow. An equation solution also offers a clearer insight into the workings of a system, as its mathematical properties are stated explicitly rather than emerging from simulated behavior.

In the Appendix we derive from first principles formulas for calculating PS under the assumptions of SDT for both Matched and Fixed Attention Window scenarios, for both equal and unequal stimulus intensities, and for any n, τ, Q, and M. To our knowledge these PS equations have not been provided before. We show how the equations can be used to simulate psychometric functions in order to see how the fitted threshold and slope parameters vary with the form of summation and the four above parameters. We discuss how the threshold and slope parameters differ between PS and AS and differ between SDT and HTT. Finally, we show how the equations can be used to fit psychometric function data from an actual experiment. For this we have conducted a binocular summation experiment, and have used the summation equations to estimate parameters such as the transducer exponent τ and to test whether AS or PS better accounts for the data.

In summary, there are two primary aims to our work. First, to reiterate some of the key differences between the SDT and HTT frameworks for modeling AS and PS, and second to derive numerical equations for modeling PS under SDT.

Modeling additive summation and probability summation

Under SDT the internal strength of a signal is denoted by d', which represents the distance between the Gaussian-distributed internal noise (denoted by N) and signal + noise (denoted by S) distributions in standard deviation, or z units. This is illustrated in Figure 3, along with some of the other parameters referred to in this section.

Additive summation

Under SDT, d' is related to stimulus strength by:

$$d' = (gs)^{\tau} \tag{1}$$

where s is the strength or amplitude of the stimulus (e.g., its contrast), g is a scaling factor that converts stimulus space into d' space and incorporates the reciprocal of the internal noise standard deviation, and τ is the exponent of the internal transducer. Under the assumptions of additive internal noise, AS can then be expressed by two equations. The first deals with stimulus components that are of equal strength:

$$d' = \frac{n(gs)^{\tau}}{\sqrt{Q}} \tag{2}$$

where n is the number of stimulus components and Q the number of monitored channels. As we noted earlier, Q can refer either to channels with different stimulus selectivities (e.g., for different orientations or spatial frequencies) or to different possible stimulus locations.

The $\sqrt{Q}$ relationship embodies the fact that when adding noise, one must add their variances, not standard deviations. If σ is the standard deviation of the internal noise for each monitored channel, the resulting σ of Q noise distributions is $\sqrt{(Q\sigma^2)}$ or $\sigma\sqrt{Q}$; in other words, σ increases with Q by a factor of $\sqrt{Q}$. Since σ is unity (d' is expressed in units of standard deviation), the expression simplifies to $\sqrt{Q}$. The relationship between n and Q determines whether one is dealing with a Matched or Fixed Attention Window scenario: if $Q = n$, it is Matched, if $Q > n$, it is Fixed.

If the stimulus components are of unequal strength, the equation is instead:

$$d' = \frac{1}{\sqrt{Q}} \sum_{i=1}^{n} (g_i s_i)^{\tau_i} \tag{3}$$

where s_i, g_i, and τ_i are the stimulus strength, gain, and transducer exponent of the ith stimulus component.

Table 1 presents the four main varieties of AS derived from Equation 2, and gives the calculation of the summation slope, which describes how detection thresholds would be expected to vary with the number of stimulus components n given the value of the exponent τ.

Typically, we wish to model psychometric functions of proportion correct detections Pc as a function of stimulus strength s. In a forced-choice task, the optimal decision rule under the assumptions of SDT, and the rule generally assumed to be employed by observers, is the MAX (maximum) rule schematized in Figure 1, which states that the observer chooses as the target the alternative or interval that produces the biggest signal. For a single stimulus, the standard SDT formula for converting Pc to d' based on the MAX decision rule is:

$$Pc = \int_{-\infty}^{\infty} \phi(t - d')\Phi(t)^{M-1} dt \tag{4}$$

(Green & Swets 1966; Kingdom & Prins, 2010; Wickens, 2002), where t is the strength of a sample signal, $\phi(t - d')$ the height of the signal distribution at t and $\Phi(t)$ the area under the noise distribution to the left of t, as shown in Figure 3. M is the number of alternatives in the forced-choice task. A detailed exposition of this formula is provided in Kingdom and Prins (2010). To obtain equations for the psychometric function for detecting multiple stimuli under AS, we substitute Equations 2 and 3 for d' into Equation 4. This gives equations for Pc as a function of s, given parameters g, τ, M, Q, and n. If we denote AS_{SDT} for the equal and $AS_{SDT}uneq$ for the unequal component stimuli situations, the two psychometric function equations can be denoted respectively by:

$$Pc = AS_{SDT}(s, g, \tau, M, Q, n) \tag{5}$$

$$Pc = AS_{SDT}uneq([s_1, s_2..s_n], [g_1, g_2..g_n], [\tau_1, \tau_2..\tau_n], M, Q) \tag{6}$$

where in Equation 6, s_1, $s_2 \ldots s_n$ are the set of different stimuli, g_1, $g_2 \ldots g_n$ their associated scaling factors, and τ_1, $\tau_2 \ldots \tau_n$ their associated transducer exponents. Both of the above functions can be fitted to a plot of Pc against s, with M, Q, and n as fixed parameters, and g and τ as free parameters to be estimated. Examples of this usage will be given later.

Equation 5 can be inverted in order to calculate s from Pc, and the resulting the function can be denoted by:

$$s = AS_{SDT}INV(Pc, g, \tau, M, Q, n) \tag{7}$$

Probability summation

"Probability summation" is somewhat of a misnomer in the context of either the SDT or HTT framework, since in neither case are the component stimulus probabilities summed. Nevertheless, we will stick with convention. The equations for PS under the assumptions of SDT provided in this section, which are the main focus of this study, have not to our knowledge been provided before. Each can be considered as a development of equation B10 in the appendix of Shimozaki, Eckstein, and Abbey (2003). Shimozaki et al. only considered the specific case of PS for two unequal strength stimuli under the Matched Attention Window scenario (our term; see our Appendix for Shimozaki et al.'s equation). Here we generalize Shimozaki et al.'s equation to accommodate a larger set of parameters. The derivation of each of the equations below is given in the Appendix, in a manner that will hopefully be accessible to the mathematical nonexpert. Both equations can be considered as the PS equivalents of Equations 2 and 3 for AS. For the equal stimulus strength situation, the equation is:

$$Pc = n\int_{-\infty}^{\infty} \phi(t - d')\Phi(t)^{QM-n}\Phi(t - d')^{n-1} dt \ldots + (Q - n)\int_{-\infty}^{\infty} \phi(t)\Phi(t)^{QM-n-1}\Phi(t - d')^{n} dt \tag{8}$$

where, as shown in Figure 3, t is sample stimulus strength; $\phi(t)$ and $\phi(t - d')$ are the heights of the noise and signal distributions at t; and $\Phi(t)$ and $\Phi(t - d')$ are the areas under the noise and signal distributions to the left of t. For the unequal component signal strength situation the equation is:

$$Pc = \sum_{i=1}^{n} \left[\int_{-\infty}^{\infty} \phi(t - d_i')\Phi(t)^{(QM-n)} \prod_{j=1, j\neq i}^{n} \Phi(t - d_j') dt \right] + (Q - n)\int_{-\infty}^{\infty} \phi(t)\Phi(t)^{QM-n-1} \prod_{j=1}^{n} \Phi(t - d_j') dt \tag{9}$$

As with the AS formulas we can substitute d' with $(gs)^{\tau}$ and formulate psychometric function equations relating Pc to s for both equal and unequal stimulus component scenarios. If we change the prefix AS to PS, the psychometric function equations for PS can be denoted as:

$$Pc = PS_{SDT}(s, g, \tau, M, Q, n) \quad (10)$$

and

$$Pc = PS_{SDT}uneq([s_1, s_2..s_n], [g_1, g_2..g_n], [\tau_1, \tau_2..\tau_n]M, Q) \quad (11)$$

The inverse of Equation 10 can be denoted by:

$$s = PS_{SDT}INV(Pc, g, \tau, M, Q, n) \quad (12)$$

The six function equations, three for AS (Equations 5 through 7) and three for PS (Equations 10 through 12) are all solvable using numerical integration. Equations 7 and 12, which convert Pc to s, require in addition an iterative search procedure.

In what follows, we demonstrate the usage of the six function equations as well as their implementations in the Palamedes toolbox (Prins & Kingdom, 2009) in two ways. First we show how they can be used to simulate psychometric functions and determine how the fitted thresholds and slopes vary as a function of n, Q, and τ, for both PS and AS. Since summation studies typically fit their data with a Weibull psychometric function (e.g., Graham, 1989), for the sake of consistency we have also fitted the simulated data with the Weibull. The Weibull function is defined as:

$$Pc = \gamma + (1 - \gamma)\left[1 - \exp\left(-\left(\frac{d'}{\alpha}\right)^{\beta}\right)\right] \quad (13)$$

where γ is the guessing rate (typically $1/M$), α the threshold at the 0.816 proportion correct level, and β the slope. We also demonstrate the usage of the equations and associated Palamedes routines for fitting psychophysical data from an actual summation experiment and show how to determine whether PS or AS gives the better account of the data.

Methods

Simulated summation psychometric functions

Data from the simulated psychometric functions were generated using Equations 5 through 7 for modeling AS, and Equations 10 through 12 for modeling PS. The equations were implemented by the following routines in the Palamedes toolbox, in corresponding order: PAL_SDT_AS_SLtoPC, PAL_SDT_AS_uneqSLtoPC, PAL_SDT_AS_PCtoSL, PAL_SDT_PS_SLtoPC, PAL_SDT_PS_uneqSLtoPC and PAL_SDT_PS_PCtoSL. All routines solve the equations using numerical integration. The Weibull fits to the simulated psychometric functions used the standard psychometric function fitting routines in Palamedes.

Real psychometric functions: binocular summation experiment

Subjects

Two of the authors, F. K. and G. S., were subjects. Both had corrected-to-normal vision.

Stimulus generation and display

The stimuli were generated by a VISAGE graphics card (Cambridge Research Systems, Rochester, UK) and displayed on a Sony Trinitron F500 flat-screen monitor (Sony Corporation, Tokyo, Japan). The monitor was gamma-corrected after calibration with an optical photometer (Cambridge Research Systems). Separate projection of the stimuli to the two eyes was achieved using the split-screen method, in which the stimuli were presented either side of the monitor screen and projected to the two eyes via a custom-built eight-mirror stereoscope with a viewing distance along the light path of 55 cm.

Stimuli

Stimuli were circular Gabor patches, with a spatial frequency of 2 cpd and bandwidth of 1.0 octave. They were in sine spatial phase, and either oriented −45° or +45° (i.e., left and right oblique). The Gabors were presented on a midgray background of 40 cd/m^2. To facilitate fixation and fusion, the stimuli were surrounded by a circular black ring 1-px wide and 4.8° in diameter. Stimuli were presented for 150 ms with a raised cosine temporal envelope.

There were three orientation combinations: (a) −45° to the left eye (*L*), right eye (*R*), and to both eyes (*Bin*); (b) +45° to *L*, *R*, and *Bin*; and (c) −45° to *L*, +45° to *R*, −45° and +45° to *Bin*. The method of constant stimuli was employed. For each subcondition seven logarithmically spaced contrasts (Michelson) were selected based on pilot studies in order to span the range 50%–100% correct. In two of the Bin conditions additional contrasts were employed to obtain a good span of the psychometric function.

Procedure

A two-alternative forced-choice (2AFC) procedure was employed in which one interval contained the target and the other a blank. There was an interstimulus interval of 250 ms and a 1-s inter-trial interval that followed each button press. The three orientation

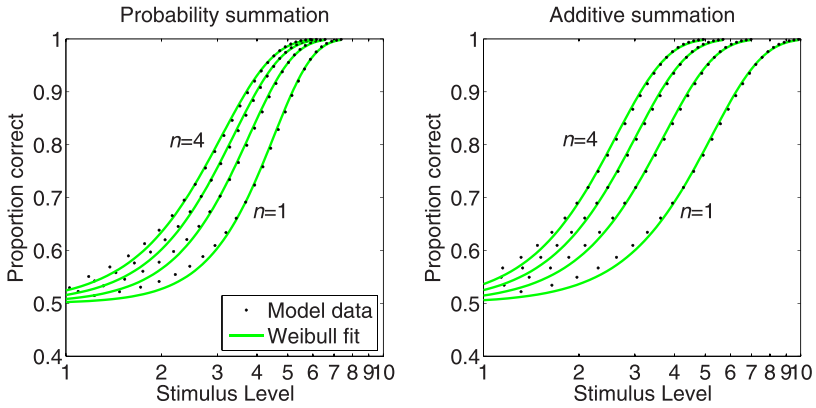

Figure 4. Simulated psychometric functions for a 2AFC task generated by the PS_{SDT} equation (left), and the AS_{SDT} equation (right), according to the Fixed Attention Window scenario with Q fixed to 4, and with a square-law transducer (i.e., $\tau = 2$). n varies from 1–4. Each function has been fitted with a Weibull function (continuous lines). As n increases the functions translate leftwards, and the slopes of the functions either decrease in the case of PS, or are constant in the case of AS The abscissa is logarithmically spaced in order to reveal how the slopes β of the fitted Weibull functions vary with n.

combinations were presented in separate sessions, but within each session, the *L*, *R*, and *Bin* conditions and contrasts were randomly interleaved, such that the observer did not know on each trial whether the stimulus was to the left eye, right eye, or both eyes. Total trials per session was 210 (3 subconditions × 7 contrasts × 10 repeats of each subcondition/contrast).

Analysis

The triplet of psychometric functions generated for each orientation combination (*L*, *R*, and *Bin*) were fitted with both PS and AS models using the PAL_SDT_Summ_MultiplePFML_Fit routines in Palamedes. The routines estimate four parameters: g_L, g_R, τ_L, and τ_R, which are respectively the scaling factors (g) and transducer exponents (τ) for the left and right eyes. Standard errors on the fitted parameters were obtained by bootstrap analysis with 200 simulations using PAL_SDT_Summ_MultiplePFML_Bootstrap-Parametric, and goodness-of-fits for each model measured using the likelihood-ratio test implemented in PAL_SDT_Summ_MultiplePFML_GoodnessOfFit, each with 200 simulations (see Kingdom & Prins, 2010). A separate analysis was conducted in which the exponent on the transducer τ was constrained to be equal in both eyes, and for this purpose customized versions of the above routines were employed.

Results

Simulated summation psychometric functions

In the following simulations, plots of *Pc* against *s* were generated using the AS and PS equations given above, each fitted with a Weibull function in order to obtain threshold α and slope β. For a standard 2AFC ($M = 2$) task, we consider how α and β vary with n, Q, and τ.

Figure 4 shows two graphs, one for PS (left) the other AS (right), each containing four simulated psychometric functions. Each psychometric function is generated from 30 linearly spaced s values, using Equation 10 for PS and Equation 5 for AS. All eight psychometric functions have input parameters $M = 2$ (and hence a guessing rate $\gamma = 0.5$ for the Weibull), $Q = 4$ and $\tau = 2$ (i.e., a square-law transducer). The variable input parameter is *n:* 1, 2, 3, and 4. By holding Q constant at 4, one simulates the Fixed Attention Window scenario, which in practice would necessitate interleaving the component stimuli such that the observer would be unable to match the attentional window to only the target stimuli mechanisms. The s values on the abscissae have been spaced logarithmically in order to reveal any differences in the slopes of the psychometric functions as a function of n.

As the graphs show, as n increases, there is a reduction in threshold α for both PS and AS simulations. The slopes β decline with n for PS, but not for AS. The decline in slope with n for PS is due to a decrease in uncertainty (Pelli, 1985): as n increases, a greater proportion of the Q monitored mechanisms become task-relevant, so fewer task-irrelevant mechanisms contribute only noise to performance. The decline in β with n is a signature property of PS under SDT for the Fixed Attention Window scenario. With AS under SDT, α varies with n, Q, and p in a straightforward manner according to the formulas in the right-hand column of Table 1. Under AS, β is invariant to both n and Q, but approximately proportional to τ.

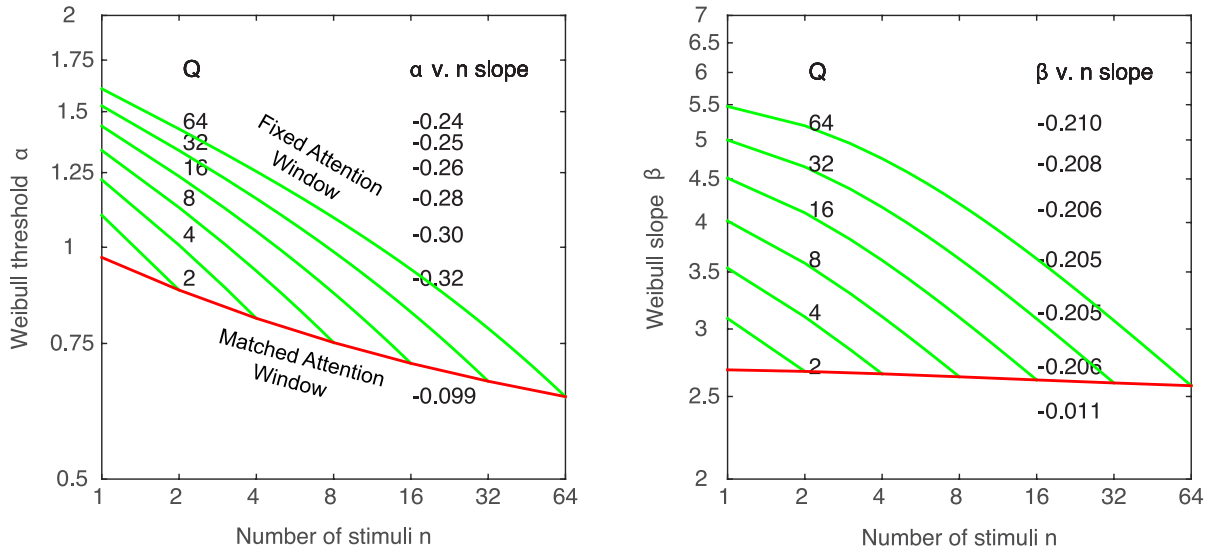

Figure 5. SDT–PS predictions from a system with a square-law transducer ($\tau = 2$) for a $M = 2$ AFC task. Green and red lines show the Fixed and Matched Attention Window scenarios respectively. The left graph shows Weibull thresholds α as a function of the number of stimuli n, for different values of Q, the number of monitored mechanisms. The α-versus-n slope values are shown aligned to each value of Q, and are the best fitting straight lines through each log–log plot. The right graph shows Weibull slopes β as a function of n and Q. The β-versus-n slope values are again from the best-fitting straight lines through the log–log data. The slopes for the Matched Attention Window are shown beneath the red lines. Note that neither graph has an equal logarithmic range on the ordinate and abscissa.

We now consider the situation for PS under SDT in more detail. Figure 5 shows how α and β varies with n and Q under PS, again for a square-law transducer ($\tau = 2$). The slopes of the α-versus-n and β-versus-n plots given for each value of Q on the graphs have been calculated from the straight-line fits to each log–log plot. The α-versus-n slopes on the left range from -0.3 for $Q = 2$ to -0.21 for $Q = 64$. The β-versus-n slopes (i.e., the "slope of the slope"—how the slope of the psychometric function changes with increasing n) on the right vary only very slightly around an average of about -0.21. If the different component stimuli are blocked and the observer is assumed to monitor only the signals from relevant mechanisms ($n = Q$), which we have termed the Matched Attention Window scenario, the predictions are the dashed lines in Figure 5. Related figures to Figure 5 can be found in Meese and Summers (2012).

The effect of the transducer exponent τ on the α-versus-n and β-versus-n slopes is shown in Figure 6. The α-versus-n slopes are approximately inversely proportional to τ, ranging between about -0.6 to -0.15 for a four-fold increase in τ from unity. The β-versus-n

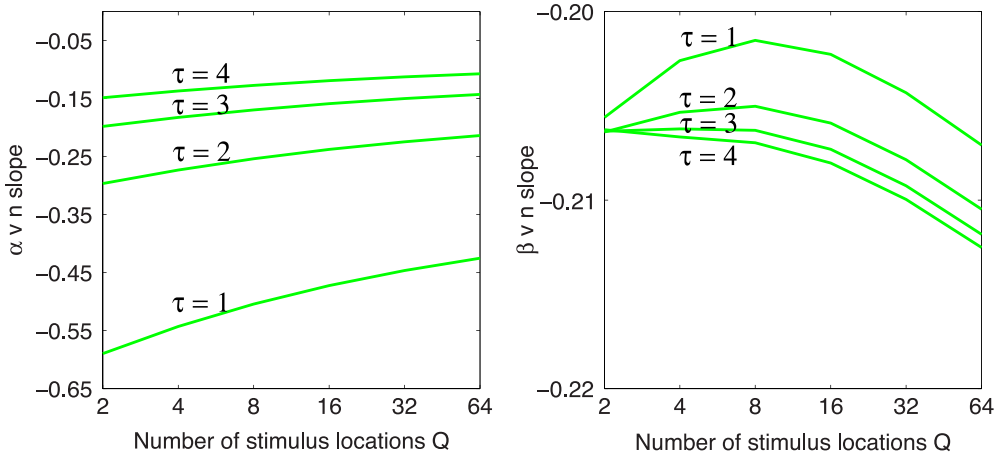

Figure 6. Effect of the transducer exponent τ on the α-versus-n and β-versus-n slopes (shown in Figure 3 when $\tau = 2$) plotted as a function of Q, the number of monitored mechanisms.

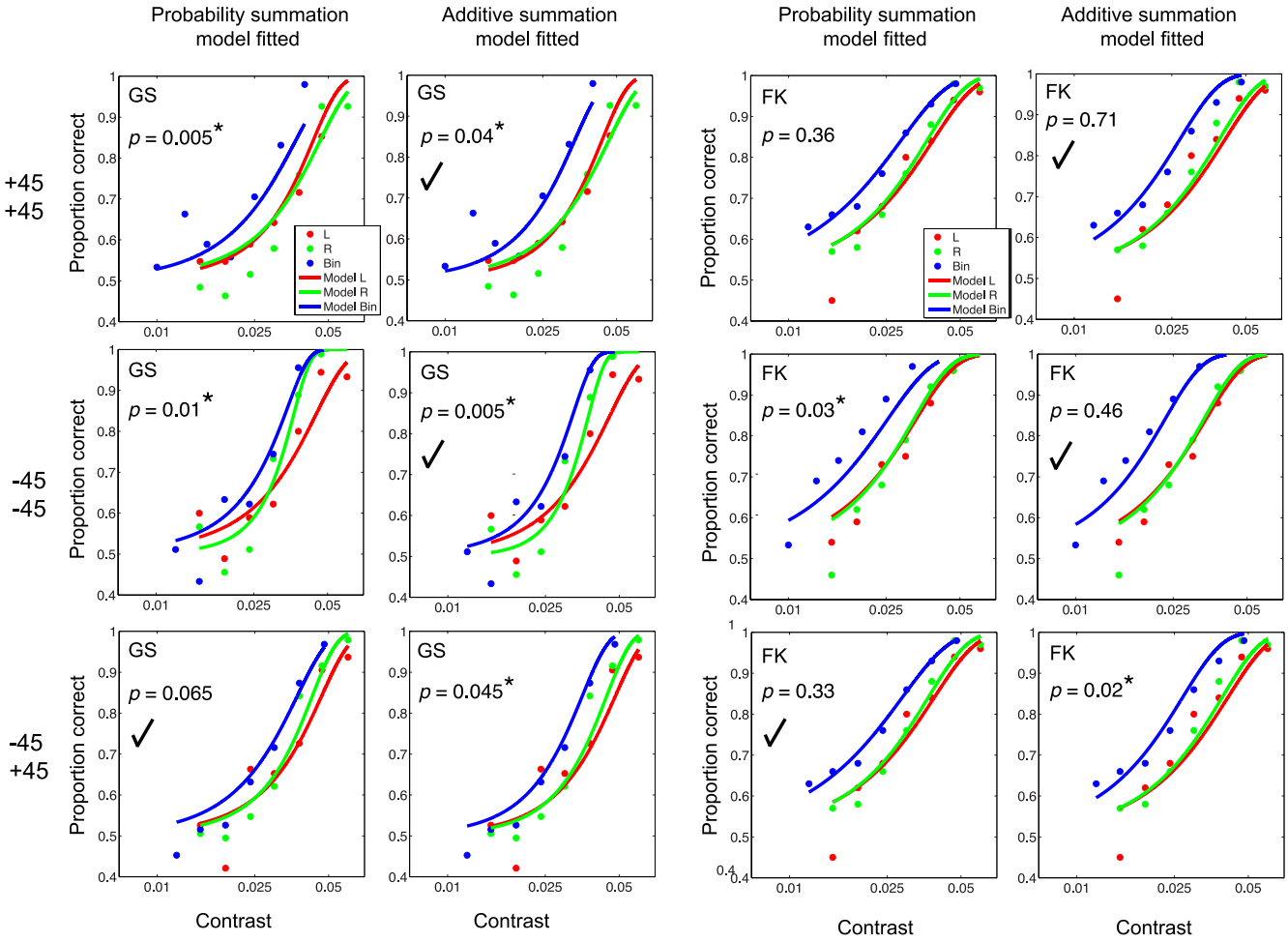

Figure 7. Results from the binocular summation experiment with summation models fitted using the multiple-fit method. Each plot shows proportion correct as a function of contrast for *L*, *R*, and *Bin* conditions (red, green, and blue circles). The three types of stimulus combination are indicated on the left with the first number indicating the *L* Gabor orientation and the second number the *R* Gabor orientation. Data for subject G.S. on the left and F.K. on the right. The *p*-value in each graph is from the transformed likelihood-ratio goodness-of-fit test, with higher *p*-values indicating better fits. A star means that the model can be rejected at the $p < 0.05$ criterion. The ticks show which of the two models gives the better fit according to AIC. See text for details and further analysis.

slopes vary little as a function of τ (or Q for that matter), being clustered around −0.21.

The predictions from the SDT–PS model can be contrasted against those of HTT. The HTT–PS model predicts no difference between the Matched and Fixed Attention Window designs. Furthermore, PS under HTT predicts no change in β with summation (Mayer & Tyler, 1986; Nachmias, 1981). The HTT–PS model uses β to predict how α should change with summation. Under the commonly used Minkowski approximation (accurate for systems with fewer than 10^4 mechanisms), the slope of the function relating $\log \alpha$ to $\log n$ is $-1/\beta$ (Quick, 1974; Robson & Graham, 1981). The AS models in Table 1 also predict no change in β with summation. For these models, however, the exponent τ provides sufficient flexibility that any α-versus-n slope can be achieved (the exponent also determines β).

In summary, the use of PS equations employing numerical integration confirm and extend the signature prediction of PS under SDT, namely that the psychometric slopes should decrease with summation in experiments where the different component stimuli are interleaved and therefore conform to the Fixed Attention Window scenario (Meese & Summers, 2012; Tyler & Chen, 2000).

Results from binocular summation experiment

The data were fit with both PS and AS models, using Equations 11 and 6 above, which incorporate respectively Equations 9 and 3. Fitting was based on a maximum-likelihood criterion, and used a multiple-fit method, in which all three psychometric functions, namely *L*, *R*, and *Bin*, were simultaneously fit with

Subject	Condition	Better model	AIC	g_L	g_R	τ_L	τ_R	*SR*
G. S.	+45+45	AS	−6.900	29.8±1.39	29.4±1.52	2.64±0.49	2.22±0.32	1.410
	−45−45	AS	−0.668	30.1±1.58	31.7±1.13	2.21±0.33	4.11±0.66	1.175
	−45+45	PS	2.142	28.0±1.50	29.4±1.47	2.03±0.32	2.36±0.33	1.175
F. K.	+45+45	AS	−4.830	44.7±2.41	41.3±2.22	2.21±0.33	2.04±0.30	1.450
	−45−45	AS	−11.900	43.3±2.31	43.0±2.42	1.78±0.23	1.92±0.29	1.620
	−45+45	PS	12.630	37.8±2.62	39.0±2.60	1.41±0.18	1.51±0.19	1.270

Table 2. Model fits to the data from the binocular summation experiment with τ free to vary between the eyes. *Notes*: The numbers defining each condition give the orientations of the Gabor patches in the left and right eyes respectively. AS = additive summation, PS = probability summation. g_L, g_R, τ_L and τ_R are the estimated parameters from the better fitting SDT model (AS or PS) together with standard errors derived from bootstrap analysis. The better model is determined by the sign of the difference in the measure of AIC.

either the PS or AS model. The fixed parameters in both models were M (number forced-choice alternatives), which was set to 2, Q (number of monitored channels) set to 2 (two eyes), and n (number of stimuli) set to 1 for the L and R psychometric functions, and 2 for the *Bin* psychometric function. Note that setting Q to 2 for all conditions follows from the fact that the L, R, and *Bin* conditions (for each orientation combination) were interleaved not blocked, thus conforming to the Fixed Attention Window scenario. The fitted parameters were g (stimulus gain) and τ (transducer exponent) for each eye, resulting in four estimates: g_L, g_R, τ_L, and τ_R. The data and model fits are shown in Figure 7, and Table 2 shows the parameter estimates together with bootstrap errors. The p-values in the plots are goodness-of-fit values calculated using the likelihood-ratio test of goodness-of-fit (Kingdom & Prins, 2010). As can be seen, many of the models can be rejected using the $p < 0.05$ criterion. It should be noted, however, that most models are likely be rejected by this criterion with sufficient number of trials, since no model is perfect (Burnham & Anderson, 2002; Prins, personal communication, January 12, 2014). An alternative to the p-value for comparing the models is Akaike's Information Criterion (AIC; Akaike, 1974), and the AS–PS AIC differences are given in Table 2. A negative AIC difference implies that the AS model is better, a positive AIC difference that the PS model is better.

Table 3 presents the results of the same analysis, but this time with the transducer exponent τ constrained to be the same in both eyes, a reasonable assumption given that the physiology of the two eyes' pathways is presumably very similar (we are grateful to Tim Meese for suggesting this model variant).

Although the relative goodness-of-fits of the PS and AS models and their AIC differences vary considerably, the results broadly agree with findings from previous studies: If the left- and right-eye stimulus orientations are the same, they combine additively, whereas if they are cross-oriented they combine probabilistically (Blake, Sloane, & Fox, 1981; Meese, Georgeson, & Baker, 2006). The estimates of the transducer exponent τ in Table 3 average to 2.5 for G. S. and 1.8 for F. K. and are close to the square-law transducer for contrast transduction found in previous studies (Heeger, 1991; Legge & Foley, 1980; Meese et al., 2006; Meese & Summers, 2009, 2012; Stromeyer & Klein, 1974).

Table 4 shows thresholds, slopes, summation ratios (*SR*s), and Minkowski summation (m) measures obtained from fitting each psychometric function separately with a Weibull. The Minkowski expression for summation is:

$$S_{cmb} = \left[\sum_{i}^{n} S_i^m\right]^{1/m} \tag{14}$$

where S_i is sensitivity to the ith stimulus component,

Subject	Condition	Better model	AIC	g_L	g_R	τ
G. S.	+45+45	AS	−6.78	30.7±1.15	28.6±0.99	2.38±0.20
	−45−45	AS	−2.21	27.2±0.91	34.5±1.08	2.91±0.39
	−45+45	PS	1.91	27.3±1.14	30.1±1.15	2.20±0.19
F. K.	+45+45	AS	−4.89	45.4±1.61	40.7±1.55	2.12±0.18
	−45−45	AS	−11.90	42.5±1.80	43.7±1.80	1.85±0.13
	−45+45	PS	12.50	37.3±1.75	39.6±1.83	1.46±0.11

Table 3. Model fits to the data from the binocular summation experiment with transducer exponent τ constrained to be the same in the two eyes. *Note*: All other parameters are the same as in Table 2.

		L		R		Bin			
Subject	Condition	α	β	α	β	α	β	SR	m
G. S.	+45+45	0.042±0.0018	3.83±0.82	0.041±0.0014	5.43±1.44	0.030±0.0014	3.27±0.69	1.41	2.03
	−45−45	0.039±0.0017	3.22±0.71	0.034±0.0012	5.65±1.49	0.031±0.011	4.87±3.6	1.16	4.60
	−45+45	0.042±0.0019	2.97±0.62	0.038±0.0014	4.19±0.84	0.034±0.0013	3.93±0.95	1.17	4.45
F. K.	+45+45	0.028±0.0011	3.48±0.75	0.030±0.0012	3.05±0.59	0.020±0.001	2.94±0.53	1.45	1.87
	−45−45	0.032±0.0014	2.83±0.53	0.031±0.0012	3.28±0.64	0.019±0.0009	2.39±0.44	1.62	1.43
	−45+45	0.034±0.0015	2.53±0.44	0.032±0.0014	3.26±0.58	0.026±0.0013	2.06±0.33	1.27	2.93

Table 4. Weibull thresholds α and slopes β, *t*s, fit to the data from the binocular summation experiment. *Notes*: *L* = left eye; *R* = right eye; *Bin* = both eyes. Also given are the summation ratios (SR) and Minkowski exponents (*m*).

S_{cmb} sensitivity to the combination stimulus, n the number of stimuli, and m the Minkowski exponent that expresses the inverse of the degree of summation (note that m is not the same as M, the number of alternatives/intervals in the forced-choice task). If we replace sensitivity in Equation 14 with the reciprocal of Weibull threshold α, Minkowski m for the binocular summation experiment can be expressed in the form:

$$\frac{1}{\alpha_{Bin}^m} = \frac{1}{\alpha_L^m} + \frac{1}{\alpha_R^m} \quad (15)$$

where α_{Bin}, α_L, and α_R are the *Bin*, *L*, and *R* thresholds, respectively. Using iterative search one can find the value of m that satisfies this equation. The *SR* is the ratio of monocular to binocular thresholds, and expresses directly how much better two eyes are compared to one. Rather than average the (log) values of *SR* obtained from the left- and right-eye monocular/binocular threshold ratios, we can calculate a single *SR* from m (we are grateful to Tim Meese for suggesting this method) using the relation:

$$SR = \sqrt[m]{n} \quad (16)$$

The calculated *SR*s for $n = 2$, as well as Minkowski m values, are given in Table 4. These values are in keeping with those reported in the aforementioned binocular summation studies, though it is worth noting that higher binocular *SR*s have been observed for some types of crossoriented stimuli, for example low spatial frequency luminance (Meese & Baker, 2011) and chromatic (Gheiratmand, Meese, & Mullen, 2013) gratings.

Summary and conclusion

It is important to emphasize that the expositions provided here make a number of assumptions: first, that the internal noise limiting detection is additive (i.e., its variance does not change with signal strength), second, that it is Gaussian, and third, that it is uncorrelated. Violations of these assumptions can reduce the predicted improvements from PS (Schwarz & Miller, 2014). For example if the internal noise affecting the component mechanisms is entirely correlated (or where the dominant noise source occurs later in the system), the system will behave in a winner-take-all manner and no improvement in performance from summation will occur.

Notwithstanding the above caveats, our new method allows a SDT–PS model to be fitted directly to the raw data from a psychophysical experiment. Because the processing time when using formulas is so much less than when using Monte Carlo simulations, it is possible to estimate relatively quickly parameters such as the stimulus gain and transducer exponent, their bootstrap errors, and the goodness-of-fit of each summation model. This means that comparisons can be made as to whether behavior conforms to AS or PS with greater statistical power than was possible before. Finally, the incorporation of a non-linear transduction term results in models with general applicability to the detection of multiple stimuli.

Keywords: probability summation, signal detection theory, high threshold theory, visual detection

Acknowledgments

This study was supported by Natural Sciences and Engineering Research Council of Canada grant #RGPIN 121713-11 and Canadian Institute of Health Research grant #MOP 123349 given to F. K. Thanks to Nicolaas Prins for his invaluable help with writing the Palamedes summation psychometric function fitting routines and to Mike Landy for many helpful comments on an earlier version of the manuscript.

Commercial relationships: none.
Corresponding author: Frederick Kingdom.
Email: fred.kingdom@mcgill.ca.

Address: McGill Vision Research, Department of Ophthalmology, Montreal, Quebec, Canada.

References

Akaike, H. (1974). A new look at the statistical model identification. *IEEE Transactions on Automatic Control*, *19*(6), 716–723.

Baldwin, A. S., Husk, J. S., Meese, T. S., & Hess, R. F. (2014). A two-stage model of orientation integration for Battenberg-modulated micropatterns. *Journal of Vision*, *14*(1):30, 1–21, http://www.journalofvision.org/content/14/1/30, doi:10.1167/14.1.30. [PubMed] [Article]

Bell, J., & Badcock, D. R. (2008). Luminance and contrast cues are integrated in global shape detection with contours. *Vision Research*, *48*(21), 2336–2344.

Blake, R., Sloane, M., & Fox, R. (1981). Further developments in binocular summation. *Perception & Psychophysics*, *30*(3), 266–276.

Burnham, K. P., & Anderson, D. R. (2002). Models versus full reality. *Model selection and multimodel inference* (2nd ed.). New York: Springer-Verlaag.

Dickinson, J. E., Han, L., Bell, J., & Badcock, D. R. (2010). Local motion effects on form in radial frequency patterns. *Journal of Vision*, *10*(3):20, 1–15, http://www.journalofvision.org/content/10/3/20, doi:10.1167/10.3.20. [PubMed] [Article]

Dickinson, J. E., McGinty, J., Webster, K. E., & Badcock, D. R. (2012). Further evidence that local cues to shape in RF patterns are integrated globally. *Journal of Vision*, *12*(12):16, 1–17, http://www.journalofvision.org/content/12/12/16, doi:10.1167/12.12.16. [PubMed] [Article]

Gheiratmand, M., Meese, T. S., & Mullen, K. T. (2013). Blobs versus bars: Psychophysical evidence supports two types of orientation response in human color vision. *Journal of Vision*, *13*(1):2, 1–13, http://www.journalofvision.org/content/13/1/2, doi:10.1167/13.1.2. [PubMed] [Article]

Graham, N. (1989). *Visual pattern analyzers*. Oxford, UK: Oxford University.

Graham, N., & Nachmias, J. (1971). Detection of grating patterns containing two spatial frequencies: A comparison of single-channel and multiple-channels models. *Vision Research*, *11*(3), 251–259.

Graham, N., & Robson, J. G. (1987). Summation of very close spatial frequencies: The importance of spatial probability summation. *Vision Research*, *27*, 1997–2007.

Green, D. A., & Swets, J. A. (1966). *Signal detection theory and psychophysics*. New York: John Wiley & Sons.

Heeger, D. J. (1991). Nonlinear model of neural responses in cat visual cortex. In M. Landy & J. A. Movshon (Eds.), *Computational models of visual processing* (pp. 119–133). Cambridge, MA: MIT Press.

Hoekstra, J., Van der Goot, D. P. J., Van den Brink, G., & Bilsen, F. A. (1974). The influence of the number of cycles upon the visual contrast threshold for spatial sine wave patterns. *Vision Research*, *14*(6), 365–368.

Kingdom, F. A. A., & Prins, N. (2010). *Psychophysics: A practical introduction*. London: Academic Press.

Laming, D. (2013). Probability summation—A critique. *Journal of the Optical Society of America A*, *30*, 300–315.

Legge, G. E., & Foley, J. M. (1980). Contrast masking in human vision. *Journal of the Optical Society of America A*, *70*, 1458–1471.

Loffler, G., Wilson, H. R., & Wilkinson, F. (2003). Local and global contributions to shape discrimination. *Vision Research*, *43*(5), 519–530.

Mayer, M. J., & Tyler, C. W. (1986). Invariance of the slope of the psychometric function with spatial summation. *Journal of the Optical Society of America A*, *3*(8), 1166–1172.

Meese, T. S. (2010). Spatially extensive summation of contrast energy is revealed by contrast detection of micro-pattern textures. *Journal of Vision*, *10*(8):14, 1–21, http://www.journalofvision.org/content/10/8/14, doi:10.1167/10.8.14. [PubMed] [Article]

Meese, T. S., & Baker, D. H. (2011). A re-evaluation of achromatic spatiotemporal mechanisms: Non-oriented filters are monocular and adaptable. *i-Perception*, *2*, 159–182.

Meese, T. S., Georgeson, M. A., & Baker, D. H. (2006). Binocular contrast vision at and above threshold. *Journal of Vision*, *6*(11):7, 1224–1243, http://www.journalofvision.org/content/6/11/7, doi:10.1167/6.11.7. [PubMed] [Article]

Meese, T. S., & Summers, R. J. (2009). Neuronal convergence in early contrast vision: Binocular summation is followed by response nonlinearity and linear area summation. *Journal of Vision*, *9*(4):7, 1–16, http://www.journalofvision.org/content/9/4/7, doi:10.1167/9.4.7. [PubMed] [Article]

Meese, T. S., & Summers, R. J. (2012). Theory and

data for area summation of contrast with and without uncertainty: Evidence for a noisy energy model. *Journal of Vision*, *12*(11):9, 1–28, http://www.journalofvision.org/content/12/11/9, doi:10.1167/12.11.9. [PubMed] [Article]

Meese, T. S., & Williams, C. B. (2000). Probability summation for multiple patches of luminance modulation. *Vision Research*, *40*, 2101–2113.

Nachmias, J. (1981). On the psychometric function for contrast detection. *Vision Research*, *21*, 215–223.

Pelli, D. G. (1985). Uncertainty explains many aspects of visual contrast detection and discrimination. *J. Opt. Soc. Amer. A, 2,* 1508–1532.

Pirenne, M. H. (1943). Binocular and uniocular threshold of vision. *Nature*, *152*, 698–699.

Prins, N., & Kingdom, F. A. A. (2009). *Palamedes: Matlab routines for analyzing psychophysical data.* Retrieved from http://www.palamedestoolbox.org.

Quick, R. F. (1974). A vector-magnitude model of contrast detection. *Kybernetik*, *16*(2), 65–67.

Quick, R. F., Mullins, Q. W., & Reichert, T. A. (1978). Spatial summation effect on two-component grating thresholds. *Journal of the Optical Society of America A*, *68*(1978), 116–121.

Robson, J. G., & Graham, N. (1981). Probability summation and regional variation in contrast sensitivity across the visual field. *Vision Research*, *21*(3), 409–418.

Rovamo, J., Luntinen, O., & Näsänen, R. (1993). Modelling the dependence of contrast sensitivity on grating area and spatial frequency. *Vision Research*, *33*, 2773–2788.

Sachs, M. B., Nachmias, J., & Robson, J. G. (1971). Spatial-frequency channels in human vision. *Journal of the Optical Society of America A*, *61*(9), 1176–1186.

Schmidtmann, G., Kennedy, G. J., Orbach, H. S., & Loffler, G. (2012). Non-linear global pooling in the discrimination of circular and non-circular shapes. *Vision Research*, *62*, 44–56.

Schwarz, W., & Miller, J. O. (2014). When less equals more: Probability summation without sensitivity improvement. *Journal of Experimental Psychology: Human Perception & Performance*, *40*(5), 2091–2100.

Shimozaki, S. S., Eckstein, M. P., & Abbey, C. N. (2003). An ideal observer with channels versus feature-independent processing of spatial frequency and orientation in visual search performance. *Journal of Optical Society of America A*, *20*, 2197–2215.

Stromeyer, C. F., & Klein, S. (1974). Spatial frequency channels in human vision as assymetric (edge) mechanisms. *Vision Research*, *14*, 1409–1420.

Tan, K. W., Dickinson, J. E., & Badcock, D. R. (2013). Detecting shape change: Characterizing the interaction between texture-defined and contour-defined borders. *Journal of Vision*, *13*(14):12, 1–16, http://www.journalofvision.org/content/13/14/12, doi:10.1167/13.14.12. [PubMed] [Article]

Tanner, W. P., & Swets, J. A. (1954). A decision-making theory of visual detection. *Psychological Review*, *61*(6), 401–409.

To, M. P., Baddeley, R. J., Troscianko, T., & Tolhurst, D. J. (2011). A general rule for sensory cue summation: Evidence from photographic, musical, phonetic and cross-modal stimuli. *Proceedings of the Royal Society B: Biological Sciences*, *278*(1710), 1365–1372.

Tyler, C. W., & Chen, C.-C. (2000). Signal detection theory in the 2AFC paradigm: Attention, channel uncertainty and probability summation. *Vision Research*, *40*, 3121–3144.

Wickens, T. D. (2002). *Elementary signal detection theory*. Oxford, UK: Oxford University Press.

Appendix

Calculation of PS under the assumptions of SDT

The basic SDT analysis makes the assumption that the noisy internal responses follow a Gaussian distribution, allowing us to use standard conversions between z values and probabilities. Figure A1 (top) shows a standard normal probability distribution in which the abscissa is given in units of standard deviation, or z units. The ordinate in the graph is probability density, denoted by ϕ. Probability density values are relative likelihoods, specifically derivatives or rates of change of probabilities. In order to convert intervals between z units into probabilities, one has to integrate the values under the curve between z values. If one integrates the curve between 0 and some value of z, the result is Φ, termed the cumulative normal. Because the total area under the standard normal distribution is by definition unity, the cumulative normal distribution ranges from 0–1. The cumulative normal gives the probability that a random variable from a standardized normal distribution is less than or equal to z.

The equation for the standardized normal distribution is:

$$\phi(z)\frac{1}{\sqrt{2\pi}}\exp\left(\frac{-z^2}{2}\right) \quad \text{(A1)}$$

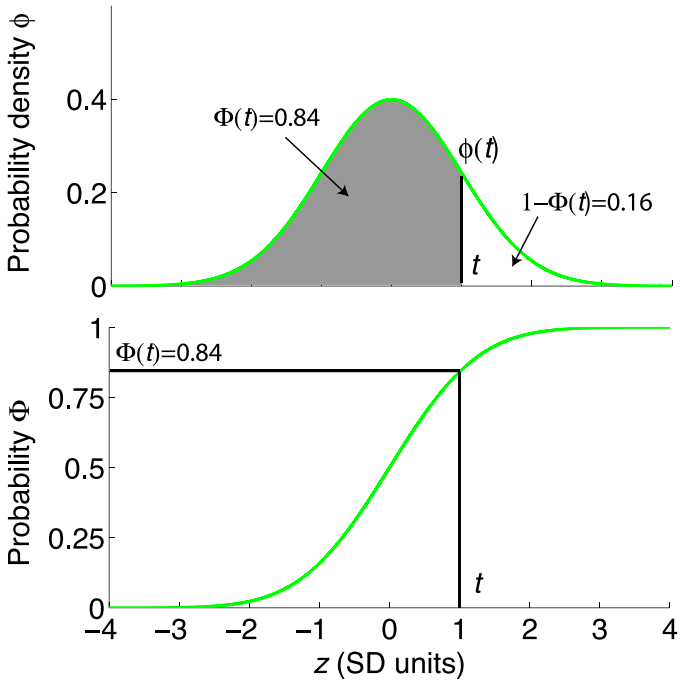

Figure A1. Top Gaussian distribution plots probability density against z in standard deviation units. The shaded area to the left of t gives the probability that t will be greater than all random samples less than t, which is 0.84 in the example shown. Bottom, cumulative probability curve, shows how this probability grows with t. Figure from Kingdom and Prins (2010), with permission.

and for the cumulative normal:

$$\Phi(z) = 0.5 + 0.5erf(z/\sqrt{2}) \quad \text{(A2)}$$

where *erf* stands for the error function, which performs the integration. The two values of 0.5 in the equation convert the range of the function to 0–1.

Measure of d'

Figure 3 in the main body of the text shows two normal distributions. The one labeled N shows the distribution of noisy internal responses to a single blank interval where no target stimulus is present. The one labeled S shows the distribution of noisy internal responses to the interval containing the target. Representing the sensory magnitudes of N and S as probability distributions means that on any trial, the actual sensory magnitudes will be random samples from those distributions. The relative probabilities of particular samples are given by the heights of the distributions at the sample points.

The mean response to the interval containing the target is higher, but the distributions still overlap. The aim of the observer in the standard forced-choice task is to identify on each trial the interval containing the target stimulus. Although the overlap means that the observer cannot be right 100% of the time, the optimal strategy to adopt would still be to select the interval with the biggest signal. This is termed the "MAX decision rule." When the target is detected by a single mechanism the performance can be calculated from the signal-to-noise ratio d' as follows:

$$Pc = \int_{-\infty}^{\infty} \phi(t - d')\Phi(t)^{M-1} dt \quad \text{(A3)}$$

where M is the number of alternatives/intervals from which the target has to be chosen (Green & Swets, 1966; Wickens, 2002). An exposition of the derivation of this equation can be found in Kingdom and Prins (2010).

Where the observer uses a MAX decision rule over multiple mechanisms, however, the prediction is more complicated. Below, we show how the relevant formulas may be derived. Our formulas can be considered as extensions of equation B10 in Shimozaki et al. (2003), which we derive below and which is itself an extension of Equation A3. One can also see parallels to our formulas in the equations for PS in Tyler and Chen (2000).

Equal stimulus intensities

First consider the Matched Attention Window scenario in Figure 2, for the case where there are two, equally detectable stimulus components, call these S_1 and S_2. Since we are dealing with PS, we assume that the two stimuli are detected by independent mechanisms, and that both mechanisms are monitored to maximize the chance of detecting the target. The number of monitored mechanisms is symbolized by Q, and the number of those that contain signal by n. The observer monitors only the relevant mechanisms, so $n = Q$.

The decision rule here is the same as for the single-stimulus M-AFC task: Select the interval/alternative with the biggest signal (i.e., the MAX rule). However, because the observer is monitoring two mechanisms, a correct decision will be made if either S_1 or S_2 produces the biggest signal. In order to calculate the expected Pc for this situation, we must first calculate the probability that S_1 will produce the biggest signal, second that S_2 will produce the biggest signal, and then add the two probabilities together. Note that for either one of the two stimuli to produce the biggest signal, a sample from it must be bigger than *both* noise signals from the null interval *and* the signal from the other stimulus in the target interval.

Taking the noise samples first, there are two on each trial. The probability that the sample t from S_1 will be greater than a noise signal is the probability that the noise signal will be less than t, which from Figure 3 is $\Phi(t)$. Thus the probability that t from S_1 will be greater than both noise signals is $\Phi(t) \times \Phi(t) = \Phi(t)^2$. By the

same argument, the probability that a sample t from S_1 will be greater than the signal from the other stimulus S_2 is $\Phi(t - d')$. To obtain the probability that the sample t from S_1 will be greater than both noise signals and the other stimulus signal, we multiply these two probabilities together: $\Phi(t)^2\Phi(t - d')$. And to obtain the probability P that a random sample t from S_1 will produce the biggest signal, we integrate this product across all values of t, taking into account the relative probability of obtaining t, which is given by its height in the stimulus distribution: $\phi(t - d')$. The result is:

$$P = \int_{-\infty}^{\infty} \phi(t - d')\Phi(t)^2\Phi(t - d')dt \quad \text{(A4)}$$

Remember, however, that there are two stimuli in the target interval, so we must include the probability that the other stimulus will produce the biggest signal. Since the probabilities that the two stimuli will produce the biggest signal are the same, we simply multiply Equation A4 by 2 to obtain the desired result. Hence:

$$P = 2\int_{-\infty}^{\infty} \phi(t - d')\Phi(t)^2\Phi(t - d')dt \quad \text{(A5)}$$

The next step is to generalize Equation A5 to any number of M and n. In general the number of noise signals in the non-target interval(s) is $n(M - 1)$, and the number of other stimulus signals in the target interval $n - 1$. Incorporating these values into Equation A5, we obtain an equation that gives proportion correct Pc:

$$Pc = n\int_{-\infty}^{\infty} \phi(t - d')\Phi(t)^{n(M-1)}\Phi(t - d')^{n-1}dt \quad \text{(A6)}$$

Equation A6 deals with the Matched Attention Window scenario, where $n = Q$. Now consider the Fixed Attention Window scenario in Figure 2, in which some of the monitored mechanisms in the target interval contain only internal noise ($n < Q$). In this case it is possible that the irrelevant noise-alone mechanisms in the target interval might produce the biggest signal, resulting in a correct decision under the MAX rule. There are Q–n noise signals in the target interval and QM-n-1 other noise signals with which each target noise signal must be compared. And there are n stimulus signals with which each noise signal in the target interval must be compared. If we follow the same logic that led us to Equation A6, the result is the second part of the equation below, which has been added to Equation A6 (with the exponent $n(M–1)$ in Equation A6 changed to $QM–n$):

$$Pc = n\int_{-\infty}^{\infty} \phi(t - d')\Phi(t)^{QM-n}\Phi(t - d')^{n-1}dt \ldots + (Q - n)\int_{-\infty}^{\infty} \phi(t)\Phi(t)^{QM-n-1}\Phi(t - d')^{n}dt \quad \text{(A7)}$$

Note that Equation A7 reduces to Equation A6 when $n = Q$. We designate Equation A7 as the general equation for computing PS under SDT for both Matched and Fixed Attention Window scenarios, when all n stimuli produce the same d'. This equation is invertable, because only a single d' value is involved; however, there is no simple solution to the inversion so it has to be implemented by an iterative search procedure.

Unequal stimulus intensities

In the case of unequal stimulus intensities, our two stimuli, S_1 and S_2 have different d' values: Call these d'_1 and d'_2. Take first again the Matched Attention Window scenario. Following the same argument as above, we begin with the probability that a sample t from S_1 will be bigger than the two noise signals in the null interval. The probability that sample t will be bigger than the one other stimulus signal is $\Phi(t - d'_2)$. Integrating across all t samples of S_1 and then adding in the corresponding integral for the probability that S_2 will provide the biggest signal, we obtain.

$$Pc = \int_{-\infty}^{\infty} \phi(t - d'_1)\Phi(t)^2\Phi(t - d'_2)dt \ldots + \int_{-\infty}^{\infty} \phi(t - d'_2)\Phi(t)^2\Phi(t - d'_1)dt \quad \text{(A8)}$$

For an M-AFC task this extends to:

$$Pc = \int_{-\infty}^{\infty} \phi(t - d'_1)\Phi(t)^{2(M-1)}\Phi(t - d'_2)dt \ldots + \int_{-\infty}^{\infty} \phi(t - d'_2)\Phi(t)^{2(M-1)}\Phi(t - d'_1)dt \quad \text{(A9)}$$

which is equation B10 in Shimozaki et al. (2003). Extending the same logic to the three stimulus case, with d's d'_1, d'_2 and d'_3 we obtain:

$$\begin{aligned} Pc = &\int_{-\infty}^{\infty} \phi(t - d'_1)\Phi(t)^{3(M-1)}\Phi(t - d'_2) \times \Phi(t - d'_3)dt \ldots \\ &+ \int_{-\infty}^{\infty} \phi(t - d'_2)\Phi(t)^{3(M-1)}\Phi(t - d'_1) \times \Phi(t - d'_3)dt \ldots \\ &+ \int_{-\infty}^{\infty} \phi(t - d'_3)\Phi(t)^{3(M-1)}\Phi(t - d'_1) \times \Phi(t - d'_2)dt \end{aligned} \quad \text{(A10)}$$

Note that as we introduce more stimuli, we increase the number of terms in each integral because there are now more stimuli with individual d' values that must be compared to each of the others under consideration. However, if we replace the right hand part of each integral with the terms containing different d' values by

the product notation, and then use the sum notation to add together the different integrals, we can generalize Equation A10 to n signals to obtain:

$$Pc = \sum_{i=1}^{n} \int_{-\infty}^{\infty} \phi(t - d_i')\Phi(t)^{n(M-1)} \prod_{j=1, j\neq i}^{n} \Phi(t - d_j')dt \tag{A11}$$

For the Fixed Attention Window scenario with unequal stimuli and Q-monitored mechanisms we apply the same logic as was applied to Equations A5 and A6. The result is:

$$Pc = \sum_{i=1}^{n} \left[\int_{-\infty}^{\infty} \phi(t - d_i')\Phi(t)^{QM-n} \prod_{j=1, j\neq i}^{n} \Phi(t - d_j')dt \right] + (Q - n) \int_{-\infty}^{\infty} \phi(t)\Phi(t)^{QM-n-1} \prod_{j=1}^{n} \Phi(t - d_j')dt \tag{A12}$$

Equation A12 thus calculates Pc for n independently detected stimuli with internal stimulus strengths d'_1, d'_2, $d'_3 \ldots d'_n$, for an M-AFC task with Q monitored mechanisms, according to the MAX decision rule under the assumptions of SDT.